

# Gas-liquid interaction in the liquid breakup region of twin-fluid atomization

U. Shavit

550

**Abstract** The interaction between air and liquid in the breakup zone of twin-fluid atomization was investigated. Using a turbulence generator, it was possible to increase the turbulence intensity without increasing the mean velocity. A comparison was made between air flows where no liquid was injected and the same flows where a liquid jet was injected and disintegrated. It was concluded that the liquid jet dominates the flow by imposing low-frequency motion to the air. The study gives ground to the interpretation that the air flow influences the liquid instability near the nozzle exit and that the balance between the influence of the initial disturbance and the downstream effects is to be searched for.

## Nomenclature

$d$	liquid jet diameter (m)
$IL$	liquid breakup length (m)
$n$	an integer
$Re$	Reynolds number ( $Re = Ud/\nu$ )
$r$	radial distance from the jet axis (m)
$U$ or $U_{liq}$	liquid velocity (m/s)
$U_{air}$	air velocity (m/s)
$U_r$	relative velocity (m/s)
$u'$	fluctuation velocity (m/s)
$\bar{u}$	mean velocity (m/s)
$We$	Weber number ( $We = \rho_l d U^2 / \sigma$ )
$\rho_l$	liquid density ( $\text{kg/m}^3$ )
$\rho_a$	air density ( $\text{kg/m}^3$ )
$\nu$	liquid kinematic viscosity ( $\text{m}^2/\text{s}$ )
$\sigma$	surface tension (N/m)
$\delta_0$	initial disturbance (m)
$\mu$	liquid dynamic viscosity (kg/ms)
$\theta_{air}$	integral time scale (s)

## 1

### Introduction

Twin-fluid atomization is a spraying technique often applied in propulsion, paint sprays, pest control, and microclimate control. The twin-fluid atomizers usually

consist of an inner tube for the liquid and an outer tube for the gas. High gas-to-liquid relative velocity results in an atomization mode which is more efficient and more controllable than pressure spraying (where no gas stream is used). Breakup length is shorter, drop size is smaller, and spray angle is wider.

The influence of the surrounding gas jet on the liquid breakup has been reported in the past (see, for example, Lefebvre 1989, Mayer 1994, Lasheras et al. 1998, Lin and Reitz 1998). The instability studies of liquid jets are usually based on the hypothesis that an initial disturbance propagates along the jet and increases its amplitude to a point of breakup and atomization. On the other hand, there are evidences that the initial disturbance concept alone can not explain the overall instability phenomena. In a recent review paper, Lin and Reitz (1998) have chosen to describe the gas-liquid interaction by writing that 'large-scale eddy structures in the gas flow impact upon the liquid jet, causing stretching, destabilization, and flapping of the liquid jet', an explanation that can be interpreted as an absolute instability. Leib and Goldstein (1986) have termed and used the concept of absolute and convective instability. Huerre and Monkewitz (1990) have reviewed such instabilities using the local/global instability classification. Convective instability describes most of the cases in which a disturbance propagates downstream the liquid surface (Lin and Reitz 1998). However, Leib and Goldstein (1986) showed that breakup can be related to absolute instability arising from a saddle-point singularity in the characteristic equation. Entov and Yarin (1984) among others have claimed that pressure fluctuations along the jet surface play an important role.

The twin-fluid breakup mechanism is affected by both the initial disturbance at the nozzle exit and the liquid gas interaction further downstream. The high gas-to-liquid relative velocity potentially increases the magnitude of the initial disturbance and augments the shear and normal stresses at the liquid interface further downstream. Entov and Yarin (1984) have shown that perturbation drift along the jet is insignificant and hence breakup is due to convective instability. They also showed that mass balance consideration requires that forces such as extension by aerodynamic drag must result in a thinning process. Therefore, breakup will occur when the thinning and bending processes overcome the stabilizing effect of surface tension. In addition to shear, normal forces reduce the liquid thickness and form thin membranes which, upon

Received: 7 March 2001/Accepted: 31 May 2001

U. Shavit  
Faculty of Agricultural Engineering  
Technion, IIT, Haifa 32000, Israel  
e-mail: aguri@tx.technion.ac.il

breakup act as the main source of small droplets. Since a complete instability analysis of twin-fluid atomization which takes into account all possible flow characteristics is unavailable, the question of whether breakup occurs due to a convective instability or due to absolute instability was left open. In other words, it is unclear whether the initial disturbance is the dominant mechanism responsible for the dramatic changes caused by the gas jet, or whether aerodynamic forces, which develop along the gas-liquid interface, are the main atomization driving force.

The general objective of the present study was to explore the interaction between the liquid jet ( $U = 1$  m/s), and the turbulent air jet ( $U_{\text{air}} = 27$  m/s) in the breakup region. If results would show that the liquid jet follows the dynamic motion of flow structures of the gas, it may be concluded that breakup occurs due to forces in the breakup zone applied on the liquid by the gas (absolute instability). In such a case, the role of the initial disturbance and its exponential growth is secondary. Under these circumstances, it is expected to find spatial and temporal similarities between the liquid jet interface and the gas flow structure. Final breakup will occur, then, due to momentum transfer through shear and normal stresses applied on the liquid jet by the velocity of the gas. On the other hand, if results show poor correlation and limited influence of the air turbulent characteristics on the liquid jet motion, the effect of the initial disturbance may prove to be important. Hence, quasi-one-dimensional convective stability analyses may be used.

The characteristics of the air flow field is required for spray modeling tasks such as prediction of the conditions for secondary breakup (critical Weber number), spray trajectories, drop coalescence, evaporation, reactive flows, turbulence spray interaction and modulation. Knowledge of the flow field near the nozzle is secondary for spray modeling if the air flow is significantly modified by the presence of the liquid jet. The 'initial plane' is located at an axial location which coincides with the breakup location and its flow characteristics are the theme of this study. The specific objectives of the study were to show that air flow can be measured accurately in the vicinity of the breakup zone, to characterize the gas flow in this region with and without the liquid jet, and to provide the detailed flow regime at the 'initial plane' of the spray. To pursue the research objectives, it was chosen to measure the air velocity and to calculate the mean velocity, rms velocity, time scale, and length scale in an axial location which coincides with the liquid jet breakup point.

The paper begins with a detailed description of the experimental setup and procedure, addressing the level of confidence in the measurements. This is followed by a discussion on results of velocity, correlation functions, and turbulence scales and their significance to the physical mechanisms of liquid twin-fluid breakup and atomization. The paper ends with conclusions and interpretation of the results.

## 2

### Experimental procedure

#### 2.1

##### Gas turbulence variations

A turbulence generator was embedded in a twin-fluid atomizer which was designed to experimentally study the effects of gas turbulence on liquid breakup and atomization (Shavit and Chigier 1996). Using this experimental atomizer, it was possible to increase the turbulence intensity without increasing the mean velocity or the Reynolds number. The operation of the atomizer was controlled by several upstream pressure regulators which affect the internal flow pattern and determine the flow conditions at the atomizer exit.

#### 2.2

##### Experimental setup

Water was supplied from a 10-l accumulator which was pressurized by house air. An alarm circuit was connected to a pressure regulator switch and was automatically turned on when the water supply pressure varied from its setting by more than 2.5%. House air was filtered, dried, and regulated by two stage pressure regulators. Upstream air pressure was measured by pressure-gauging systems, one for the main flow and one for the transverse flow. The reading error associated with three reading stages was  $\pm 0.05$  kPa (for a range of 0–14 kPa),  $\pm 0.7$  kPa (14–70 kPa), and  $\pm 3.4$  kPa (70–420 kPa). The air flow was seeded with propylene glycol using a TSI six-jet atomizer. Seeding particle mean diameter was about  $3 \mu\text{m}$ , resulting in a Stokes number of approximately  $10^{-5}$ . A symmetric manifold was used to divide the air into four transverse tubes. The experimental atomizer was connected to a three-directional positioner with a maximum location error of  $\pm 13 \mu\text{m}$  in one horizontal direction and  $\pm 100 \mu\text{m}$  in the other two directions.

A two-component TSI Argon-ion laser Doppler velocimeter (LDV) was used to measure air velocities (TSI Inc. 1982). Frequency shift of 40 MHz was applied by the Bragg cells, while 1 MHz for the axial velocity component and 5 MHz for the other component were chosen from the down mixer. In order to achieve high signal quality and high data rate, an on-axis forward-scatter mode was chosen. Electronic gain was typically around one and the frequency band was kept as broad as possible. A data collection rate of 10 kHz gave repeatable results with low sensitivity to operational parameters such as gain, filtering, laser power, and N-cycle. In some of the experiments, a coincidence mode with a time window of  $20 \mu\text{s}$  was used to measure the two velocity components simultaneously.

Special operational conditions were applied when temporal and spatial correlation functions were obtained. For the calculation of temporal auto-correlation function, the LDV setup and the flow seeding concentration were such that a maximum of 100 kHz data rate was obtained. For the calculation of spatial correlation functions, the dual-beam LDV system was modified such that instead of two perpendicular velocity components, two axial velocities

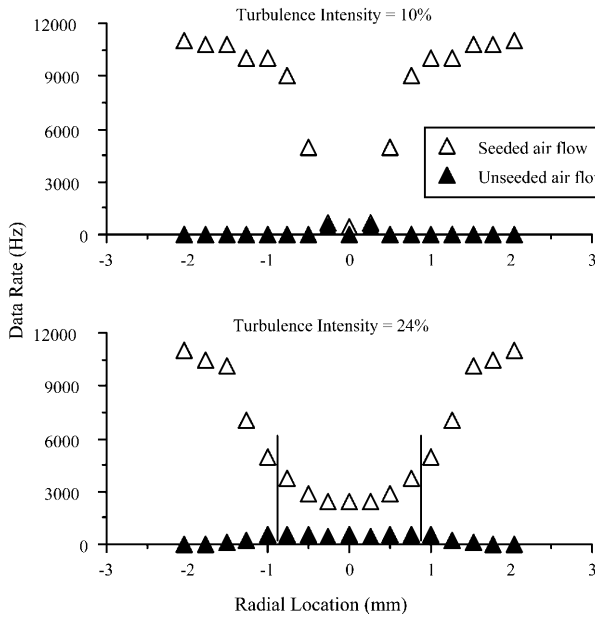


Fig. 1. The LDV data acquisition rate when the liquid jet is surrounded by seeded air and un-seeded air

(parallel to each other) were measured simultaneously. The two color laser beams were directed through only one optical channel such that both measured the axial velocity component. By fine alignment of the mirrors, it was possible to create two optical probes which are a small measurable distance apart from each other. The optical probes were translated horizontally to measure the lateral correlation function and vertically for the longitudinal correlation. For each translation, the receiving optical alignment was adjusted so that the signal could be detected through the system pin hole. A maximum possible span between the probes was  $930\ \mu\text{m}$  in the lateral direction and  $1105\ \mu\text{m}$  in the axial direction. Both velocities were measured simultaneously by applying the coincidence mode, with a time window of  $20\ \mu\text{s}$  and a relative lower data rate of 6 kHz.

### 2.3

#### Level of confidence in the measurements

The discrimination between air and liquid flows in the liquid breakup region is a non-trivial experimental task. Under the experimental conditions, the space where liquid was found was restricted to the near-axis region. This region contains large individual drops, ligaments, and often the far edge of the intact liquid jet. Even without choosing a signal amplitude discrimination mode, the LDV often rejects large liquid particles due to signal saturation. The level of confidence in the air velocity measurements when liquid is present was tested by examining the LDV data acquisition rate as was recorded under two experimental conditions. In both test conditions, the liquid jet was present. Seeding, however, was added to the air in only one of the two tests. Figure 1 shows that the data acquisition rate ratio between seeded and un-seeded air indicates that when air turbulence intensity is 10% or 17%, an unacceptable degree of ambiguity in the measurements is

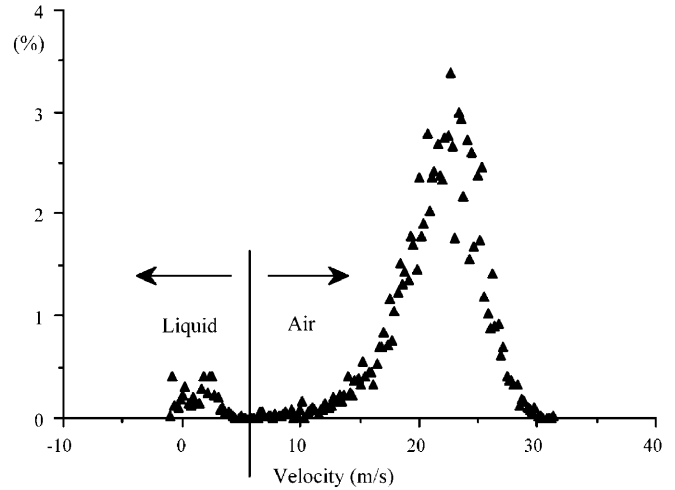


Fig. 2. Velocity bi-modal histogram as was measured by the LDV for air flow (mean flow 27 m/s and 10% turbulence intensity) at  $r = 0.25\ \text{mm}$ . Axial location coincides with the liquid breakup length

restricted to a radius of only 0.25 mm. Where the air turbulence intensity is 24%, the high ambiguity in the measurements is restricted to a radius of 0.75 mm. Velocity histograms were plotted so that the existence of bi-modal and near-bi-modal velocity histograms could be detected (see Fig. 2). Bi-modal velocity histograms were detected only in the region where the level of uncertainty was identified earlier as unacceptable (0.25 mm for 10% and 17% turbulence intensity and 0.75 mm for 24% turbulence intensity). Computations of mean and rms velocities and spatial and temporal correlation functions were based on the histogram portion which represents the air flow only.

### 3

#### Results and discussion

Flow visualization of the liquid jet under a variety of air flow conditions is shown in Fig. 3. A comparison between a thin laminar water jet injected into quiescent environment (Fig. 3a) and the same water jet injected coaxially into a high-velocity gas jet demonstrates the strong influence of the air stream. Figure 3d, b, and c show the same water jet injected coaxially into an air jet with a mean velocity of 27, 39, and 53 m/s, respectively. The breakup of low-velocity liquid in stagnant air is symmetric. It occurs many diameters away from the nozzle and generates a drop size in the order of magnitude of the jet diameter. As shown, the liquid-jet breakup by high air velocity involves highly unsteady asymmetric core motion and generates a drop size which can be three orders of magnitude smaller than the jet diameter (Lefebvre 1989, Shavit 1994, Lasheras et al. 1998, Kufferath et al. 1999).

Air velocity profiles were obtained for the flow conditions visualized in Fig. 3d–f. Average air and liquid velocities were 27 m/s and 1 m/s, respectively, for all three cases. The flow conditions differ from each other in air turbulence intensity (10%, 17%, and 24%). Turbulence was varied by changing the axial-to-transverse flow rate ratio inside the atomizer, while maintaining a constant overall

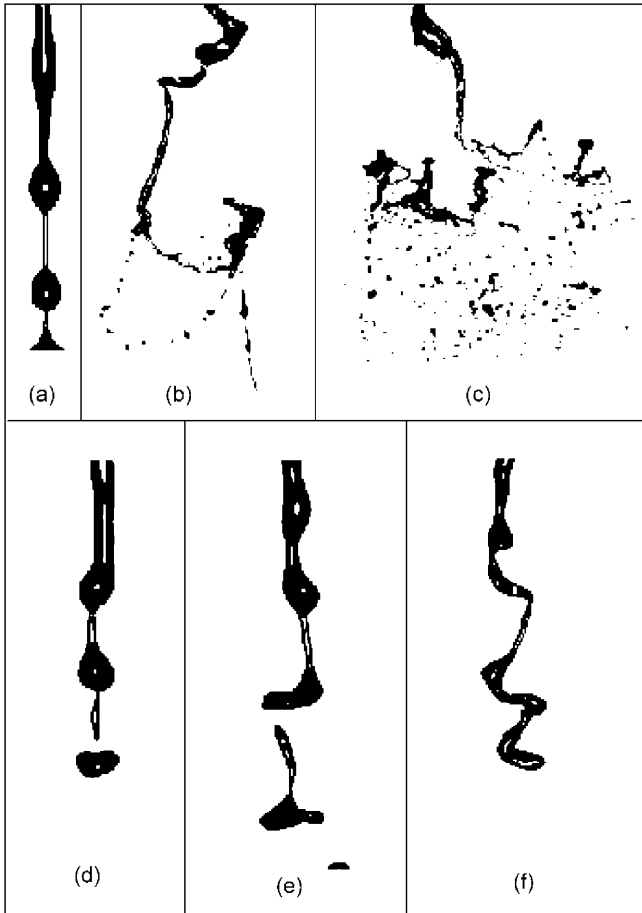


Fig. 3a–f. Flow visualization of the breakup region. Liquid velocity is  $U_{\text{Liq}} = 1$  m/s for all cases. a Rayleigh's symmetric mode; b  $U_{\text{air}} = 39$  m/s; c  $U_{\text{air}} = 53$  m/s; d  $U_{\text{air}} = 27$  m/s, turbulent intensity is 10%; e  $U_{\text{air}} = 27$  m/s, turbulent intensity is 17%; f  $U_{\text{air}} = 27$  m/s, turbulent intensity is 24%

flow rate (Shavit and Chigier 1996). The most visualized effect of air turbulence is the increasing lateral motion. The jet dynamics become less symmetric, its breakup length is shorter, and the liquid ligaments shape is more complex. Such liquid-jet dynamics was described by Yarin (1993) as 'bending instability'. According to the stability analysis developed by Entov and Yarin (1984), high relative velocity between the gas and the liquid may cause an 'overturning' of the jet. The jet geometry of their prediction is in an excellent agreement with the breakup visualization shown in Fig. 3f. Liquid bending and 'overturning' was also demonstrated by high-speed cinematography in our laboratory. It was indicated that 'overturning' of the liquid results in normal interaction between the liquid and air, which causes the formation of thin membranes followed by their breakup and the formation of small droplets.

The liquid lateral motion is expected to influence the air flow. Mean velocity of the single-phase air jet and mean velocity of the same air jet when liquid was injected, are shown in Fig. 4. The axial distance of the measurement from the nozzle exit coincides with the average axial distance,  $IL$ , of the liquid breakup point (24.7 mm, 22.6 mm, and 17.7 mm under turbulence conditions of 10%, 17%,

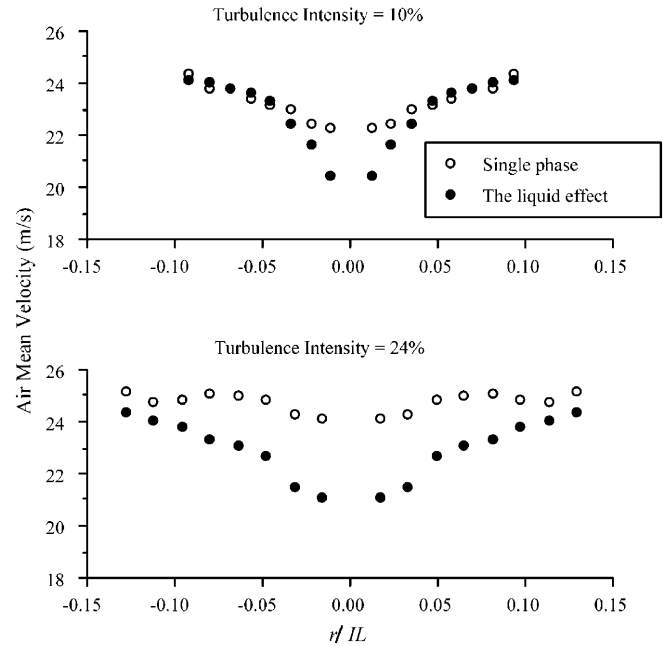


Fig. 4. The influence of the liquid jet on the axial mean air velocity

and 24%, respectively). The turbulence generator was designed and tuned such that profiles of mean air velocity are very similar to each other, while their turbulence intensity is different (Shavit and Chigier 1996). This is the case at the nozzle exit, as well as further downstream. As expected, the interaction between the liquid and the air results in a decrease of mean air velocity at the vicinity of the jets axis. Figure 4 shows that the relative change in air velocity increases with air turbulence intensity. Considering the nearest point to the jet axis, the change in the low and high turbulent flows is 8.3% and 12.8%, respectively. It was also observed that when turbulence intensities of 10% and 17% were tested, the velocity decrease was limited to a radial range of about 1 mm. When turbulence intensities of 24% were tested, the velocity decrease was found to extend beyond a radius of 2 mm. The radial distance for which changes in air mean velocity were detected is similar to the lateral amplitude of the liquid-jet motion (Shavit 1994). As shown in Fig. 3, higher turbulence forces more liquid ligaments to overturn and form a perpendicular orientation to the main flow direction. The radial liquid spread and the change in orientation contribute to the slowing-down effect of air shown in Fig. 4.

When no air stream is used (Fig. 3a), the liquid breakup length,  $IL$ , normalized by the liquid-jet diameter,  $d$ , can be calculated by the linear theory using the Reynolds number,  $Re$ , and the Weber number,  $We$ , (Rayleigh 1892, McCarthy and Molloy 1974, Reitz and Bracco 1986),

$$IL/d = \text{Ln}(d/\delta_0) \left\{ \sqrt{We} + 3We/Re \right\} \quad (1)$$

The Reynolds number is  $Re = Ud/\nu$  and the Weber number is  $We = \rho_1 d U^2 / \sigma$ , where  $U$  is the liquid velocity,  $\rho_1$  is the liquid density,  $\nu$  is the liquid viscosity, and  $\sigma$  is surface tension. The normalized breakup length,  $IL/d$ , under the current conditions was measured and found to be 75.3.

Applying Eq. 1 results in  $\ln(d/\delta_0) = 14.4$  and an initial disturbance of  $\delta_0 = 5.57 \times 10^{-10}$  m, which is in a good agreement with previous studies (Grant and Middleman 1966).

The initial-disturbance concept has been often used to analyze liquid instability for cases other than the Rayleigh mode (Crapper et al. 1975, Rangel and Sirignano 1988, Lin and Ibrahim 1990, Yang 1992, Li and Kelly 1992, and Yarin 1993, among others). Yarin (1993), for example, used the initial-disturbance concept and analyzed the stability of liquid jets exposed to transverse, 'bending', disturbances. Under such conditions, the liquid breakup length is

$$\frac{IL}{\Delta} = \left[ \frac{3\mu\rho_l d^2 U_r^3}{4(\rho_a U_r^2 - 2\sigma/d)^2} \right]^{\frac{1}{3}} \quad (2)$$

where  $\mu$  is liquid viscosity,  $U_r$  is relative velocity,  $\rho_a$  is air density, and  $IL/\Delta$  is the breakup length,  $IL$ , normalized by  $\Delta = \ln(nd/\delta_0)$  with  $n$  as an integer ( $n = 1$  or  $2$ ) and  $\delta_0$  as the initial disturbance. It is clear that Eq. 2 does not consider the effect of turbulence intensity. However, breakup length measurements can be used to estimate the initial disturbance,  $\delta_0$ . Employing Eq. 2 on the measured breakup length results in an initial disturbance of  $2 \mu\text{m}$ ,  $3.6 \mu\text{m}$ , and  $14.2 \mu\text{m}$  for turbulence intensity conditions of 10%, 17%, and 24%, respectively. Namely, if Eq. 2 is applicable, the role of the air turbulence is in increasing the amplitude of the initial disturbance  $\delta_0$ .

The influence of the liquid jet on the air rms velocity is shown in Fig. 5. No or little change in air turbulence intensity would support the assumption that the liquid follows the dynamics of the gas. Such an assumption is most likely to be rejected due to the vast differences in the phases density. However, spatial analysis (Shavit and

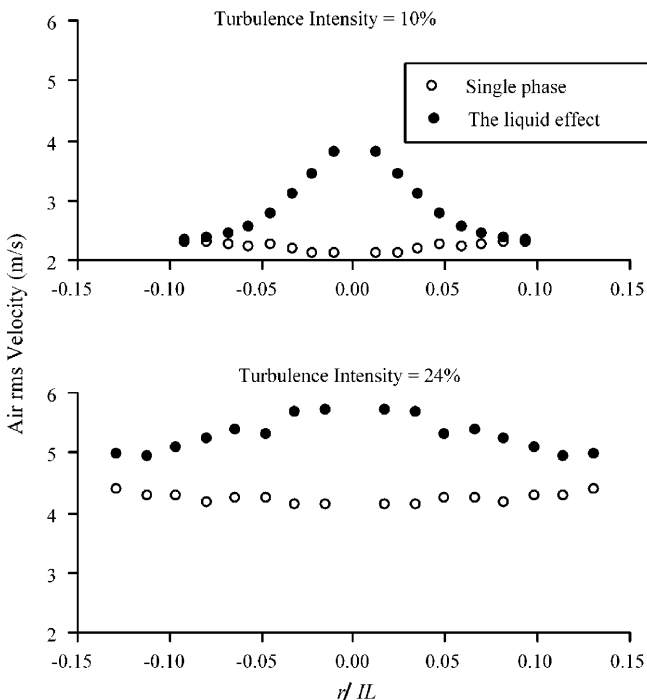
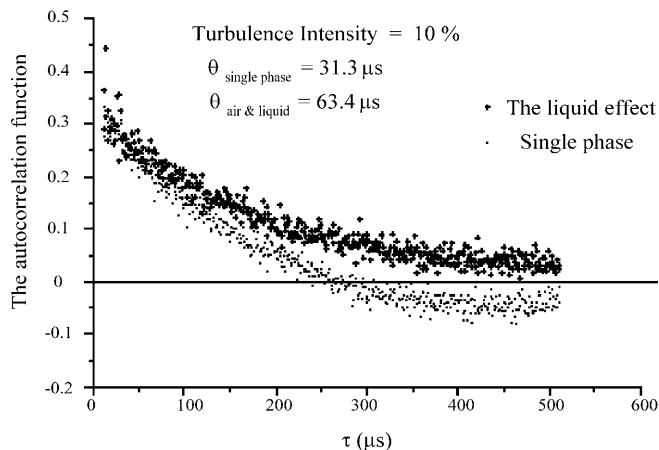


Fig. 5. The influence of the liquid jet on the axial rms air velocity

Chigier 1995) discovered similarities between the geometrical structure of the liquid interface in the breakup zone and the spectrum of length scales in the air. Results of the current study show (Fig. 5) that the lateral and axial flapping motion of the liquid jet serves as a major source for air turbulence. The turbulence intensity increases because of wakes which were developed behind the moving liquid structures. In addition, the liquid jet adds a 'wall' effect, which results in high local shear, contributing to the production of turbulence. To support the conclusion that turbulence is produced by the dynamics of the liquid jet and not only by the 'law of the wall', a simple calculation was made. Based on results from Fig. 4, velocity gradient,  $\partial u/\partial r$ , was calculated for high- and low-turbulence air flows. At a radial distance of 0.5 mm (second point from the center), the velocity gradient is  $4.3 \times 10^3$  1/s in the low-turbulence flow, and  $3.6 \times 10^3$  1/s in the high-turbulence flow. As a first approximation, we follow the Prandtl theory and calculate the rms velocity using  $\sqrt{u'^2} \approx k\partial\bar{u}/\partial r$ .  $u'$  is the fluctuation velocity,  $\bar{u}$  is the mean velocity,  $r$  is the radial distance from the jet axis, and  $k = 0.4$ . The calculation shows that if we assume that the 'wall' (the liquid jet) is the only source for turbulence increase, the contribution of the liquid to the rms velocity is expected to be 0.75 m/s in both air flows. Figure 5 shows that the increase in rms velocity is higher and reaches a value of about 1.5 m/s. Parthasarathy and Faeth (1990) studied the generation of turbulence by interaction of glass spheres with nearly stagnant water and stagnant air. Their findings indicate that even when the particles Reynolds number is low, high turbulence intensities are generated. Despite the vast differences in the liquid structures of the two studies, the conclusion made by Parthasarathy and Faeth (1990) agrees well with the results of the current study. Figure 5 also demonstrates the ability of the turbulence generator to generate uniform profiles of high turbulence intensities. The high velocity fluctuations, which are generated inside the atomizer, did not dissipate. They maintained more than 60% of their intensity. Figure 5 shows that the radial range, over which air rms velocity is affected, is larger when turbulence intensity is higher. On the other hand, the absolute increase in air rms velocity is similar in all the three flows (about 2 m/s at the jet center). This finding is in good agreement with the finding that the time correlation function of the motion of the liquid jet and the corresponding integral time scales are not sensitive to variations in the air turbulence (see the power spectral density functions described herein and in Shavit 1994). Both the differences in the radius of influence and the similar 2-m/s increase in the rms velocity indicate that in the breakup region, temporal interactions between the liquid and the air are dominated by the motion of the liquid jet; In the time domain, the air flow in the breakup region is influenced by the liquid jet much more than the liquid is affected by the air flow.

The time history of the air velocity signal was measured and the air flow time auto-correlation functions were calculated. These measurements were obtained in the liquid breakup region for the single-phase air jet and for the case where liquid was present (Fig. 6). Auto-correlation functions were calculated for each of the air flow condi-



**Fig. 6.** Temporal auto-correlation function as influenced by the presence of liquid. Measurements were taken for air flow of 10% turbulence intensity, at a radial location of 0.5 mm and axial location which coincides with the breakup length. Similar auto-correlation functions were calculated for each of the air flow conditions and along radial distances up to 2 mm from the jet axis

tions and along radial distances of up to 2 mm from the jet axis. The air auto-correlation functions with the presence and absence of the liquid jet were identical for radial distances of more than 1.75 mm. When no liquid was injected and where the measurements radial location was closer to the jet axis, the value of the auto-correlation functions was low. In a previous publication (Shavit 1994), the air flow was measured at the nozzle exit and the time auto-correlation function was calculated. It was found that turbulence intensity decreases the value of the air auto-correlation function. It was also found that the decrease is significant in the high frequencies and that there is little difference in the low frequencies. In Fig. 6 we show the effect of the liquid jet on the auto-correlation coefficients. It is shown that the liquid presence reduces the auto-correlation coefficients in the low-frequency range rather than in the high-frequency range. Where an increase in turbulence intensity involves generation of high-frequency small-size eddies for energy dissipation, the influence of the liquid on the air flow is most dominant by a low-frequency phenomenon which is associated with the motion of the liquid jet.

The characteristics of liquid interface waves were studied and reported by several authors. These studies analyzed liquid sheets (Arai and Hashimoto 1985, Mansour and Chigier 1991) and liquid jets (Arai and Hashimoto 1986, Eroglu and Chigier 1991). The analysis presented by Arai and Hashimoto (1986) was based on an assumed linear velocity profile in the surrounding air with its thickness as a parameter. They have shown that the velocity gradient in the air affects the jet stability. This conclusion is relevant to the differences in turbulence generated by our atomizer. As turbulence increases, the velocity gradient at the liquid interface increases. Arai and Hashimoto (1986) also concluded that there is a critical relative velocity (around 25 m/s) above which the asymmetric behavior replaces the symmetric one. Hence, our flow conditions are within the asymmetric mode defined

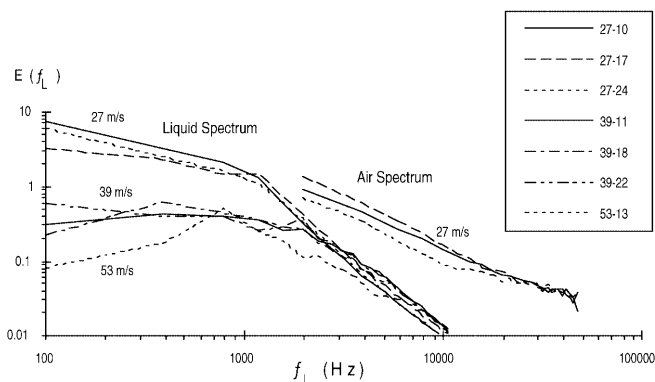


**Fig. 7.** Temporal power spectral densities of the liquid jet motion and the air turbulence. Liquid spectrum is for air average velocities of 27 m/s, 39 m/s, and 53 m/s. Air spectrum is for air average velocity of 27 m/s only. Liquid spectrum was measured at an axial location upstream from the breakup point, where the signal was the best. Air spectrum was calculated based on velocity measurements at the nozzle exit. The numbers used in the legend box represent the mean velocity (m/s) and the turbulence intensity (%)

by these authors. They demonstrated a helical wave propagation and measured the vibration frequency of the jet, which was found to be around 150 Hz. This peak frequency was observed in an axial distance upstream from the region of breakup. They were not able to identify a dominant frequency in the breakup region itself.

For a general comparison between the time characteristics of the gas flow and the liquid jet, a power spectral density function was computed and is presented in Fig. 7. The spectrum of the gas flow was calculated based on velocity measurements at the nozzle exit. Liquid measurements represent an axial location upstream from the breakup point (where data quality was the best for spectral analysis). The most notable result is the order of magnitude difference between the frequency range (and decay rate) of the air in comparison with that of the liquid. The influence of air flow rate is such that the spectrum density is lower with a maximum value at an increasing frequency (around 100 Hz, 400 Hz, and 800 Hz for air velocity of 27 m/s, 39 m/s and 53 m/s, respectively). This result is in agreement with the vibration frequency reported by Arai and Hashimoto (1986). Another important result is that turbulence intensity alone decreases the spectrum value by only a small amount.

Calculation of the air integral time scales inside the breakup region is shown in Fig. 8. The injection of liquid causes a dramatic increase in the air integral time scales. The liquid causes the air to fluctuate at lower frequencies, but with higher rms velocities. The increase in time scale can be explained by a comparison between the temporal spectral density in the single-phase air jet and the spectral density of the liquid jet flapping motion (Fig. 7). Such a comparison indicates that the time scales in the single-phase air jet are a magnitude of order smaller than the time scales of the liquid dynamic motion. The increase in air time scales, as shown in Fig. 8 is another indication that in the liquid breakup region, the motion of the liquid jet is dominant. The relative slow motion of the liquid jet

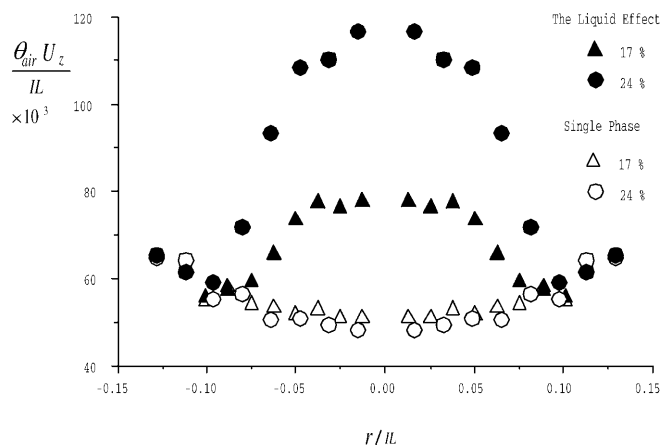


Fig. 8. The air integral time scales,  $\theta_{air}$ , as influenced by the presence of the liquid jet. Measurements were taken at an axial location which coincides with the breakup length,  $IL$ .

forces the air to follow its motion, increasing its time scales. Figure 8 also shows that when the integral time scale,  $\theta_{air}$ , is normalized by the liquid breakup length,  $IL$ , and the mean air axial velocity,  $U_{air}$ , the single-phase time scales show self-similarity (Note that  $IL$  decreases with increase in turbulence intensity). The self-similarity vanishes when the liquid jet is added. Self-similarity, which is a known property of free turbulent jets (fully developed, though) (Wynanski and Fiedler 1969, among others) is broken by the motion of the liquid jet. As shown, the liquid jet, surrounded by highly turbulent air flow (24%), causes a larger change in the air integral time scale than the less turbulent air flow. It was shown in Figs. 4 and 5 that the liquid jet introduces more changes to the air flow when its turbulence intensity is 24% than when it is 10%. This can be explained by the more significant 'overturning' behavior of the jet under high turbulence intensity (Fig. 3f).

The effects of the liquid jet on the air spatial correlation functions were also studied. It was found that the liquid jet causes, in all flows, a small decrease in the spatial correlation functions. A small increase in length scales with air turbulence intensity, which was observed when liquid was present, is similar to the increase in length scales, as was found in the single-phase flow, near the nozzle exit as well as at the breakup point. The liquid jet reduces the effective space in which turbulent structures can be developed. This may be an explanation for the decrease of the air integral length scales.

#### 4

#### Conclusions

The effect of the liquid-jet flapping motion on the surrounding air flow in the breakup region of twin-fluid atomization was studied. These effects were analyzed experimentally using an LDV. It was shown that when droplets are large and the lateral motion of the liquid is narrow, LDV can measure the velocity of the seeded air.

Results show that near the jet axis, drag between the liquid and air causes a small decrease in the air mean velocity. Despite the small change in mean velocity, it was

found that the lateral and axial flapping motion of the liquid jet serves as a major source for air turbulence. The increased turbulence, represented by the high value of rms velocity, is characterized by smaller integral length scales and larger integral time scales.

Our understanding of the breakup mechanism is as follows: gas liquid interaction generates an initial disturbance at the nozzle exit. This disturbance increases with air turbulence intensity. Instability results in an increasing wave amplitude and an 'overturning' of the liquid jet. Continuity considerations and drag between the gas and the liquid causes a thinning of the jet. The motion of the jet is governed by the initial interaction with the gas and the inherent instability. The low-density gas flow does not impose its dynamics on the liquid jet, meaning that liquid breakup is not due to absolute instability. However, once a right angle forms between the gas stream and the liquid, strong normal forces blow up the liquid to generate thin membranes. Large ligaments, rims, and membranes experience secondary breakup and generate a wide range of drop sizes.

The objective of the study was to examine the interactions between the liquid and the air jets inside the breakup zone. Results show that in the breakup zone, the temporal behavior of the air flow is influenced by the liquid jet more than the liquid is affected by the air flow. The strong influence of the air on the initial instability is to be searched for near the atomizer exit rather than in the breakup zone. The role played by the liquid jet is supported by more than one observation: the temporal behavior of the liquid jet is not very sensitive to the degree of air turbulence; the radial distance in which changes of the air flow were measured is the same as the value of the amplitude of the lateral vibration of the liquid jet; where a general increase in turbulence involves the generation of high-frequency small-size eddies for energy dissipation, the influence of the liquid-jet motion on the air flow is most dominant due to a low-frequency phenomenon which is associated with the relative slow motion of the liquid jet. Since the only change was the injection of the liquid jet, one possible interpretation of the results is a transfer of energy from the gas phase to the liquid jet. However, more research is needed, since energy dissipation, energy redistribution, pressure fluctuations, and a combination of all the mechanisms are possible.

#### References

- Arai Y; Hashimoto H (1985) Behavior of gas-liquid interface on liquid film jet (instability of a liquid film jet in a co-current gas stream). *Bull JSME* 28: 2652-2659
- Arai Y; Hashimoto H (1986) Helical surface instability of cylindrical liquid jet in co-current gas stream. *Bull JSME* 29: 77-82
- Crapper GD; Dombrowski N; Pyott GAD (1975) Kelvin-Helmholtz wave growth on cylindrical sheets. *J Fluid Mech* 68: 497-502
- Entov VM; Yarin AL (1984) The dynamics of thin liquid jets in air. *J Fluid Mech* 140: 91-111
- Eroglu H; Chigier N (1991) Wave characteristics of liquid jets from airblast coaxial atomizers. *Atomization Sprays* 1: 349-366
- Grant RP; Middleman (1966) Newtonian jet stability. *AIChE J* 15: 669-681
- Huerre P; Monkewitz PA (1990) Local and global instabilities in spatially developing flows. *Annu Rev Fluid Mech* 22: 473-537

- Kufferath A; Wende B; Leuckel W** (1999) Influence of liquid flow conditions on spray characteristics of internal-mixing twin-fluid atomizers. *Int J Heat Fluid Flow* 20: 513–519
- Lasheras JC; Villermaux E; Hopfinger EJ** (1998) Break-up and atomization of a round water jet by a high-speed annular air jet. *J Fluid Mech* 357: 351–379
- Lefebvre AH** (1989) *Atomization and sprays*. Hemisphere, Washington, D.C.
- Leib SJ; Goldstein ME** (1986) Convective and absolute instability of a viscous liquid jet. *Phys Fluids* 29: 952–954
- Li HS; Kelly RE** (1992) The instability of a liquid jet in a compressible air stream. *Phys Fluids A* 4: 2162–2168
- Lin SP; Ibrahim EA** (1990) Instability of a viscous-liquid jet surrounded by a viscous gas in a vertical pipe. *J Fluid Mech* 218: 641–658
- Lin SP; Reitz RD** (1998) Drop and spray formation from a liquid jet. *Annu Rev Fluid Mech* 30: 85–105
- Mansour A; Chigier N** (1991) Dynamic behavior of liquid sheets. *Phys Fluids A* 3: 2971–2980
- Mayer WHO** (1994) Coaxial atomization of a round liquid jet in a high speed gas stream: A phenomenological study. *Exp Fluids* 16: 401–410
- McCarthy MJ; Molloy NA** (1974) Review of stability of liquid jets and the influence of nozzle design. *Chem Eng J* 7: 1–20
- Parthasarathy RN; Faeth GM** (1990) Turbulent dispersion of particles in self-generated homogeneous turbulence. *J Fluid Mech* 220: 515–537
- Rangel RH; Sirignano WA** (1988) Nonlinear growth of kelvin-helmholtz instability – effect of surface tension and density ratio. *Phys fluids* 31: 1845–1855
- Rayleigh L** (1892) On the instability of a cylinder of viscous liquid under capillary force. *Philos Mag* 34: 145–154
- Reitz RD; Bracco FV** (1986) Mechanisms of breakup of round liquid jets. In: Chermisnoff N (ed) *The Encyclopedia of Fluid Mechanics*. Gulf Publishing, Houston, Tex., pp 233–249
- Shavit U** (1994) The effects of air turbulence and dynamic surface tension on air assist atomization. Ph.D. Thesis. Carnegie Mellon University, Pittsburgh, Pa
- Shavit U; Chigier N** (1995) Fractal dimensions of liquid jet interface under breakup. *J Atomization Sprays* 5: 525–543
- Shavit U; Chigier N** (1996) Development and evaluation of a new turbulence generator for atomization research. *Exp Fluids* 20: 291–301
- TSI Inc.** (1982) Laser Doppler velocimeter signal processor, Model 1980B instruction manual. TSI Inc., St. Paul, Minn.
- Wynanski I; Fiedler H** (1969) Some measurements in the self-preserving jet. *J Fluid Mech* 38: 577–612
- Yang HQ** (1992) Asymmetric instability of a liquid jet. *Phys Fluids A* 4(4): 681–689
- Yarin AL** (1993) *Free liquid jets and films: hydrodynamics and rheology*. Longman Scientific & Technical, Harlow, UK